Waxing and waning volcanism along the East Pacific Rise on a millennium time scale

Marie-Hélène Cormier
William B.F. Ryan
Anjana K. Shah
Wen Jin
Lamont-Doherty Earth Observatory of Columbia University, Palisades, New York 10964, USA
Albert M. Bradley
Dana R. Yoerger
Woods Hole Oceanographic Institution, Woods Hole, Massachusetts 02543, USA

ABSTRACT

Microbathymetric maps of the southern East Pacific Rise reveal subtle field relations between volcanic features and provide new insight on seafloor spreading processes. Along one of the shallowest and broadest sections of ridge at 17°28′S, lavas have erupted from a fissure system and flooded the axis through a network of lava tubes and lava channels. Along the neighboring ridge segment at 18°15′S, the axial area has subsided and formed a broad tectonized trough. A swath of newly accreted crust has since widened that trough; late-stage volcanism consists of small circular pillow mounds. We propose that these contrasting eruptive styles reflect the waxing and waning phases of a common magmatic evolution spanning a few millennia.

Keywords: East Pacific Rise, high-resolution bathymetry, volcanism, lava flows.

INTRODUCTION

Most of the volcanism on Earth occurs along the mid-ocean ridges at 2000–4000 m water depth. Multibeam bathymetry maps and side-scan sonar mosaics acquired from ships successfully delineate individual volcanic systems on scales of a few to tens of kilometers, but their resolution is insufficient to characterize individual lava flows and their associated eruptive vents. More detailed investigations have relied on observations and sampling from manned submersible and deeply towed instruments. These methods provide limited coverage along one-dimensional survey tracks and make it difficult to evaluate the field relations between subtle volcanic features such as flow fronts, eruptive fissures, lava channels, pillow mounds, or fissure swarms. Remotely operated vehicles and autonomous underwater vehicles (AUV) now make it possible to produce comprehensive maps of the seafloor that highlight these features with a precision equivalent or superior to that readily available for land studies (Chadwick et al., 2001; Johnson et al., 2002). We present results from an expedition using the AUV *ABE* (autonomous benthic explorer) that acquired very high resolution maps of the axis of the East Pacific Rise. In combination with submersible observations and sampling performed during the same cruise (Sinton et al., 2002), these data shed new light on eruptive processes along the East Pacific Rise, and suggest that the upper oceanic crust is organized in narrow ridge-parallel corridors emplaced during alternating waxing and waning magmatic phases.

MAPPING VOLCANIC SYSTEMS ALONG THE EAST PACIFIC RISE

The East Pacific Rise is the fastest-spreading mid-ocean ridge (70–150 mm/yr), and frequent volcanic activity is expected along its axis (Macdonald, 1982; Perfit and Chadwick, 1998). It is characterized for thousands of kilometers by a ridge 5–15 km wide and 300–500 m high (Fig. 1). A plateau half to several kilometers wide marks the summit of this elongated high, and glassy, mostly unsedimented lava flows occur along its length. One of the shallowest and broadest sections of the East Pacific Rise occurs at 16.5°–18.5°S and it is inferred to have benefited from an abundant magma supply over the past few 10,000 yr (Cormier et al., 1996). While the axial high in this area maintains a nearly constant depth (2620 ± 30 m), notable variations

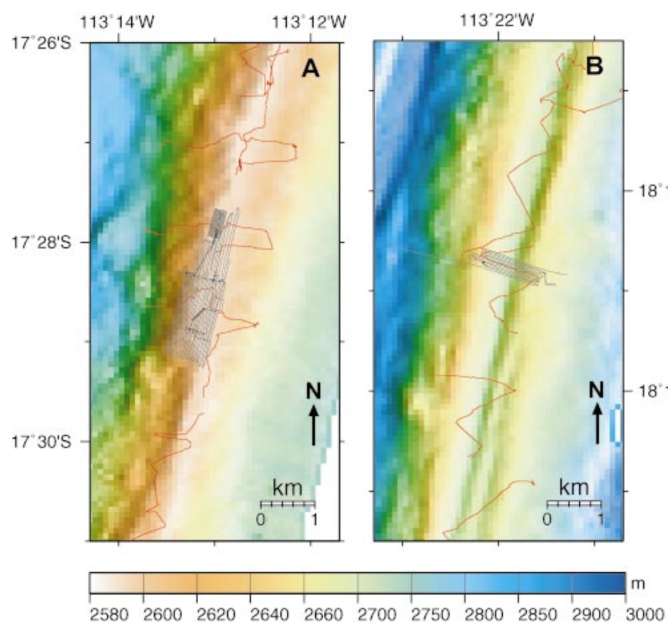

Figure 1. Contrasting morphology at two study sites based on shipboard multibeam bathymetry. Black lines indicate survey tracks from autonomous underwater vehicle *ABE.* Red lines indicate dive tracks from *NAUTILE* and *ALVIN* submersibles; these provide observational control along most of ridge axis (Auzende et al., 1996; Sinton et al., 2002). A: Axial high north of 17°56′S is smooth dome. B: Axial high at 17°56′–18°35′S is notched by an ~1000-m-wide, 50–100-m-deep trough.

in morphology suggest that accretionary processes are not uniform (Fig. 1). North of a 3 km offset of the ridge axis at 17°56′S, the axis is defined in cross section by a smooth dome. Elongated troughs <100 m wide and 12 m deep occur occasionally at the axis of the summit plateau and are too narrow to be detected via shipboard multibeam bathymetry (Auzende et al., 1996; Embley et al., 1998; Renard et al., 1985). In contrast, between 17°56′ and 18°35′S, the summit plateau is notched by a larger tectonized trough, 500–2000 m wide and 50–110 m deep (Lagabrielle and Cormier, 1999).

Submersible dives identified several eruptive units with distinctive flow morphologies and geochemistry between 17° and 19°S (Auzende et al., 1996). A 1999 expedition targeted a few of these units for detailed volcanological investigation with the submersible *ALVIN* (Sinton et al., 2002). The AUV *ABE* was deployed as an additional nighttime program and acquired near-bottom geophysical data along precisely navigated, closely spaced survey tracks (Yoerger et al., 2000). *ABE*'s deployments focused on two areas of contrasting morphology and produced microbathymetric maps of the neovolcanic zone with a resolution sufficient to identify individual flows and their vent source (Fig. 1).

VOLUMINOUS FISSURE ERUPTION AT 17°28′S

Submersible investigations between 17°20′ and 17°35′S mapped a sediment-free lava flow extending 18.5 km along axis, known as the Aldo-Kihi flow, which probably erupted within the past few decades (Auzende et al., 1996; Embley et al., 1998; Sinton et al., 2002). Troughs ~10 m deep mark the shallowest, central portion of the flow. These are drained lava lakes, as indicated by the thin roof remnants overhanging along their rims and the lava pillars within them. These drained lava lakes cluster between 17°26′ and 17°29′S, describing in plan view a system of en echelon, ridge-parallel elongated troughs (White et al., 2000). We targeted that particular area for *ABE* deployments and mapped 3 km of the neovolcanic zone with a resolution never achieved before in such a setting (Fig. 2).

The microbathymetry precisely outlines the system of en echelon drained lava lakes, including the lava pillars within them. Each elongated lava lake is 200–700 m long, to 70 m wide, and 5–12 m deep (Fig. 2A). Their rims are at the shallowest elevations in the surveyed area, confirming that they include the eruptive vents for the Aldo-Kihi lava flow. The surface of the surrounding lobate flows is exceptionally flat, sloping at 3° or less away from the vents. Two types of channelized lava flow, both ~10–40 m wide, disrupt this monotonous surface. South of 17°27′9″S (Figs. 2C, 2D), the lobate surface is interrupted where the thin roofs of subsurface lava tubes have collapsed 4–5 m down. Four such lava tubes breach the western rim of the drained lava lake system and branch downslope into an arterial pattern, feeding lava lobes 200–400 m across. The coalescence of these lobes accounts for the bulbous character of the seafloor west of the axis. New lobes overlap older lobes, producing a shingled pattern of stacked lobes. Between 17°27.7′ and 17°27.9′S, a tributary network of open lava channels spills across the west flank of the ridge axis (Figs. 2A, 2E). These channels initiate outside the drained lava lakes and widen downslope as they merge with each other. They are at most 2 m deep, and photomosaics collected by *ABE* indicate that they are floored by sheet flows whose striated surfaces follow the channel contours (Ryan et al., 1999). Striated sheet flows grade smoothly into the surrounding lobate flows, suggesting that both lava morphologies were emplaced concurrently. The floor of the open lava channels has a steeper gradient than that of the exposed lava tubes (Fig. 2F), and submersible observations show that channels carried lavas further away than tubes (Sinton et al., 2002).

The en echelon left-stepping pattern of the drained lava lakes most likely reflects the arrangement of the underlying segmented dike that

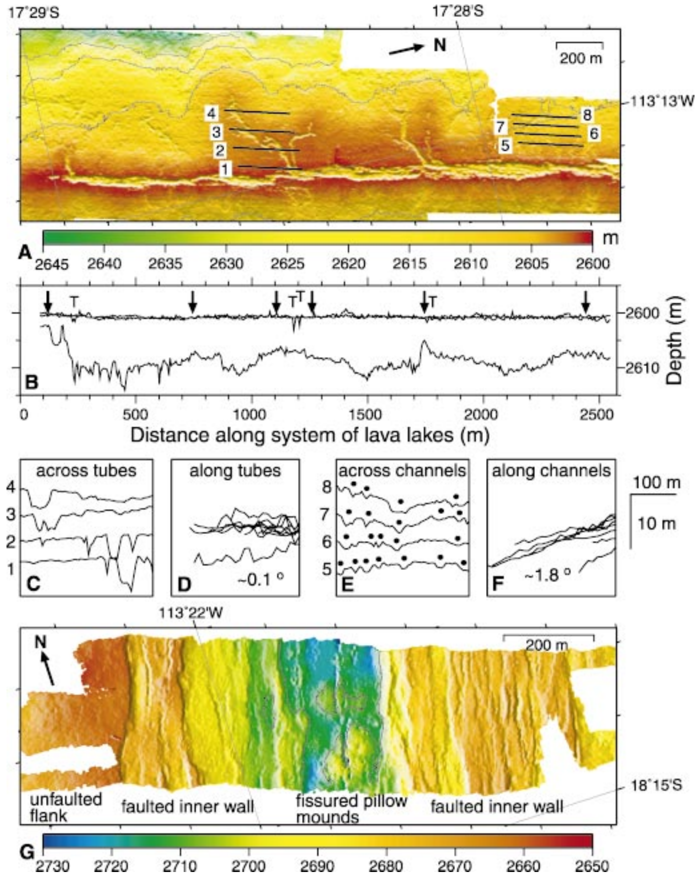

Figure 2. High-resolution bathymetry acquired along axial crest with autonomous underwater vehicle *ABE*. A: Microbathymetry outlines system of drained lava lakes that formed above en echelon feeder dike. Area is located in Figure 1A. Contour interval on ridge flanks is 10 m. B: Depth profiles measured along drained lava lakes. Two profiles centered on 2601 m correspond to west and east rims, and lower profile corresponds to deep axis of lakes. T indicates branching of lava tubes and arrows mark ends of each lava lake. Lower panels: Bathymetry profiles taken along and across channelized lava flows. Transverse profiles are located in A, scale bars are indicated at right. C and D: Lava tubes are detected where their roofs have collapsed. They diverge downslope, feeding broad lava lobes within summit area. Their floors are subhorizontal. E and F: Dots mark crossings of lava channels. Lava channels are not as deep and flow on steeper slopes than lava tubes. G: Microbathymetry near 18°15′S. Area is located in Figure 1B. 2710 m depth contour (black line) highlights inner trough and two fissured pillow mounds.

fed the eruption (Fig. 2A). Each drained lava lake strikes 13°–16°, consistent with both the N013° spreading-normal direction and the dominant N012° fault azimuth on the ridge flanks between 16° and 19°S (Cormier et al., 1996). The rims of every lava lake section as well as the top of the lava pillars within them are precisely 2601 ± 0.5 m deep (Fig. 2B): hence, the lava lake sections were probably connected during the eruption, and the height reached by the erupting lavas was controlled by hydrostatic pressure (265 bar). Such constant depth precludes that any posteruption vertical motion (as might result from downdropping of the trough floor along a set of bounding faults) has affected the rise crest, and we interpret the series of drained lava lakes as the surface expression of a single fissure eruption. Each lava lake is widest and deepest in its center and tapers near its extremities (Fig. 2A), suggesting that magma influx was at a maximum near the centers of the dike segments. The absence of levees surrounding the drained lava lakes, the lava tubes, and the lava channels (Figs. 2B, 2C, 2E) indicates that the surface of the lavas solidified early in the eruption and that magma continued to flow beneath the frozen carapace, gradually inflating the surface of the flow. Sustained influx of magma contributed to pond lavas directly above the segmented feeder dike, while a short distance away, solidifying lavas progressively built up rims that contributed to contain the erupting lavas above the vents. Submersible observations of the drained lava lakes indicate that their walls are occasionally draped with folded sheet flows, and their floors are covered with sheet flows lineated parallel to their long axis (Sinton et al., 2002). We interpret these lava morphologies to record the last stage of the eruption, when ponded lavas rapidly drained back and flowed along the bottom toward the center of the underlying feeder dike, and lavas just emplaced over the rims cascaded back down into the draining lava lakes.

The most conspicuous relief on the surface of the Aldo-Kihi lava flow results from the collapse of the thin lobate crust, and large void spaces may underlie that crust. This hypothesis is consistent with the pattern of near-bottom magnetic anomalies detected with *ABE* (Shah et al., 2003). The dimensions of the collapse windows provide clues about the thickness of the lava flow (Figs. 2B, 2C). Assuming that the lava tubes did not erode their substrate, their depths of 4–5 m provide a minimum estimate of the lava flow thickness. If the maximum depth of the lava lake system (12 m) indicates the base level of the lava tubes that drained these lakes, it provides a maximum estimate of the lava flow thickness. Hence, the ''negative'' topography of the Aldo-Kihi lava flow suggests that it is 5–12 m thick.

DECLINING ERUPTIVE ACTIVITY AT 18°15′S

Robust magmatism has probably characterized the notched axial high between 17°56′ and 18°22′S within the past 10 k.y. (Scheirer and Macdonald, 1993; Cormier et al., 1996). Direct evidence includes the common occurrence of sedimented sheet flows and lava pillars on the outer flanks of the 50–60-m-deep, 1000–1400-m-wide summit trough, and extensive fields of hydrothermal chimneys, active and inactive, lining the floor of that trough (Auzende et al., 1996; Sinton et al., 2002). The pervasive hydrothermal activity (Baker and Urabe, 1996; Marchig et al., 1986) is consistent with the existence of a magma lens ~1.5 km beneath the axis (Hooft et al., 1997). In places, drained lava lakes containing 10–15-m-high lava pillars mark the axis of the trough (Auzende et al., 1996; Sinton et al., 2002). The floor of the trough maintains a depth of 2710 ± 15 m between 18°10′ and 18°22′S (Lagabrielle and Cormier, 1999). Subsidence of the trough along its bounding faults is expected to produce larger depth variations over a distance of 20 km, and this uniform depth suggests the occasional flooding by lava flows extending most of the segment length. Nonetheless, several factors suggest that magmatism has declined for the past few millennia. The magma lens beneath that segment is 300–400 m deeper than the magma lens for the two surrounding segments (Hooft et al., 1997). Individual lava flows emplaced most recently along this segment amount to 0.3%–18% of the volume of the Aldo-Kihi flow erupted along the neighboring segment (Sinton et al., 2002). The trough is intensely faulted and fissured, and the sediment cover, although uneven, reaches a few centimeters (Auzende et al., 1996; Sinton et al., 2002). Estimated sedimentation rates are 0.3–2.6 cm/k.y. (Marchig et al., 1986; Dekov and Kuptsov, 1992), implying that lava flows have not uniformly resurfaced the floor of the trough for at least several centuries.

ABE microbathymetry data acquired across a 400-m-wide corridor near 18°15′S reveal that the seafloor deepens ~60 m toward the axis in a series of fault steps, each 10–20 m high (Fig. 2G). The floor of the inner trough is 200 m wide and relatively flat. It is occupied by two circular pillow mounds 10 m and 15 m high. These pillow constructions are only lightly sedimented and represent the latest volcanic products (Sinton et al., 2002). Fissures 6–10 m wide, in places as deep as 15 m, cleave each mound. These probably opened above dikes that failed to erupt at the seafloor. The rather large dimensions of these fissures imply either the intrusion of several shallow dikes beneath the mounds, or further dilation in response to the regional extensional regime.

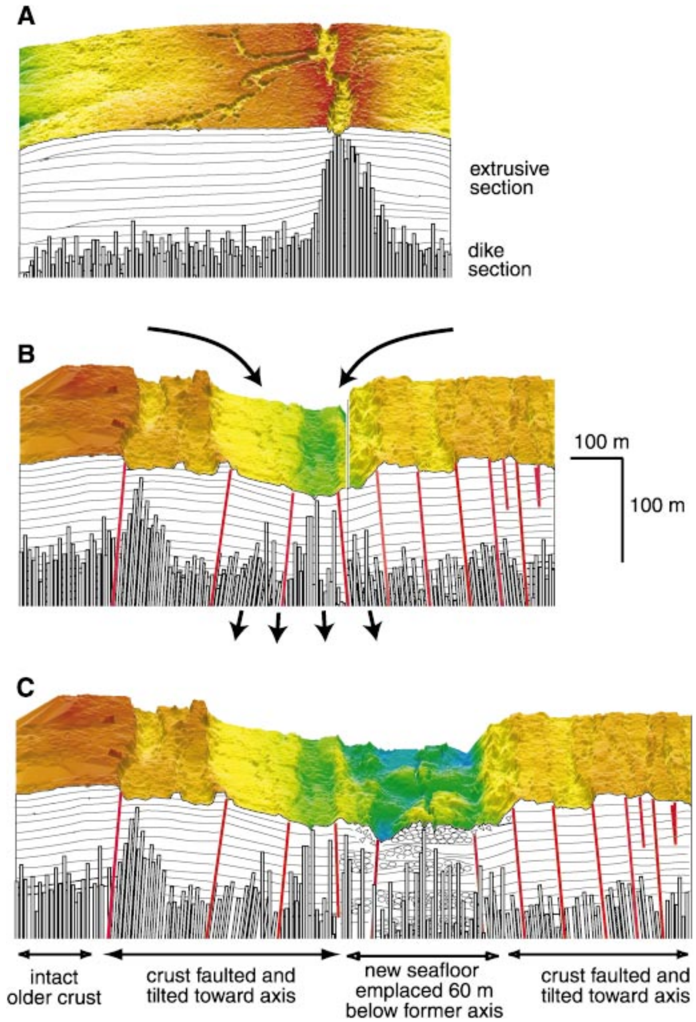

Figure 3. Evolutionary model for portions of East Pacific Rise characterized by overall robust magmatism. Cross sections are based on maps in Figure 2. A: Waxing magmatism results in voluminous fissure eruptions, as near 17°28′S. B: Waning magmatism together with sustained seafloor spreading lead to decreasing size of subjacent magma reservoir and subsidence of summit plateau (as symbolized by arrows) along series of faults (in red). C: Persistent waning conditions lead to accretion of swath of seafloor that is deeper than former ridge crest, as near 18°15′S. Eruptive products are confined within trough and consist of pillow mounds intercalated with lobate flows. Resumption of waxing conditions would result in filling of trough and development of axial morphology similar to that in A.

Combined with direct observations, *ABE*'s fine-scale bathymetry enables the sequence of eruptive and tectonic events that shaped the summit trough to be assembled. The staircases of fault blocks descending to the trough floor are sedimented, confirming that their formation predates volcanism within the inner trough. While the uniform base level (~2710 m) of the inner floor suggests the occasional flooding of the entire segment by effusive lavas, these flows erupted 60 m below the level of the former summit plateau, indicating a loss in magmatic pressure head. A waning magma supply would contribute to lower the magmatic head in several ways. As melt supply wanes, the overpressure needed to produce an eruption would build up more slowly. As a result, ultrafast spreading conditions may be accommodated with an increasing number of diking events that stop short of erupting, producing instead open fissures at the seafloor. In turn, the pervasive fissuring of the extrusive section would decrease the lithostatic load above the magma reservoir and thus lower the level to which magma can rise during an eruption. Furthermore, vigorous hydrothermal circulation through the fissured overburden would contribute to cool the upper crust and freeze the top of the magma reservoir. Altogether, feedback between the different processes would result in lavas being emplaced at greater depths until the magma supply waxes again. If the 200 m width of the inner trough represented seafloor accreted since the formation of the summit trough, this width allows determination of an upper boundary for the trough's age. Considering the local spreading rate of 142 mm/yr (Cormier and Macdonald, 1994), the inner trough may have formed ~1400 yr ago.

STRIPED CRUSTAL ARCHITECTURE AT FAST SPREADING RIDGES?

We interpret the contrasting characteristics of the neovolcanic zones at 17°29′S and 18°15′S to reflect different stages of a common magmatic evolution for ridge segments characterized by a time-averaged robust magmatism. During a waxing phase, inflationary lobate flows are dominantly erupted and most dikes reach the seafloor (Fig. 3A). During a waning phase (Fig. 3B), the neovolcanic zone becomes increasingly fissured and eventually collapses to form a large summit trough (Lagabrielle and Cormier, 1999). A chaotic stratigraphy develops as the volcanic section fractures and tilts toward the axis of accretion and subsequent dikes intrude that tilted volcanic section. The bounding walls of the summit trough act to confine subsequent eruptions, preserving the volcanic stratigraphy characteristic of waxing conditions on the flanks of the axial high (Fig. 3C). Many dikes do not erupt and the swath of new seafloor is pervasively fissured. This scenario is supported by observations at Hess Deep, where vertical exposures of a 1 Ma crustal section show dikes tilted toward the active ridge axis and crosscut by more recent subvertical dikes (Hurst et al., 1994). Provided that at least 2 k.y. elapse between waxing and waning episodes (as is inferred from the sediment cover), crustal sections with distinctly different volcanic stratigraphy will be accreted over time, resulting in a crustal architecture arranged along ridge-parallel corridors at least 500 m wide. The systematic variability in fault density, lava flow porosity, and thickness of the extrusive layer associated with waxing and waning phases may control many of the processes active on a segment scale along the East Pacific Rise including the pattern of hydrothermal circulation and the nucleation of ridge-parallel abyssal hills a few kilometers off axis. Microbathymetric and photographic surveys that extend to the base of the axial high and up various escarpments exposing the volcanic stratigraphy would provide a useful test of this crustal structure model.

ACKNOWLEDGMENTS

We thank A. Duester and R. Catanach for their assistance with *ABE* deployments, and the officers and crew of the R/V *ATLANTIS* for efficient ship operation. We thank J.M. Sinton and R. Batiza for letting us piggyback on their expedition and inviting us to participate in *ALVIN* dives. We thank W.W. Chadwick and another reviewer for constructive criticisms. This research was supported by National Science Foundation grant OCE-9730813. Lamont-Doherty Earth Observatory contribution 6421.

REFERENCES CITED

Auzende, J.-M., Ballu, V., Batiza, R., Bideau, D., Charlou, J.-L., Cormier, M.-H., Fouquet, Y., Geistdoerfer, P., Lagabrielle, Y., Sinton, J.M., and Spadea, P., 1996, Recent tectonic, magmatic, and hydrothermal activity on the East Pacific Rise between 17°S and 19°S: Submersible observations: Journal of Geophysical Research, v. 101, p. 17,995–18,010.

Baker, E.T., and Urabe, T., 1996, Extensive distribution of hydrothermal plumes along the superfast spreading East Pacific Rise, 13°30′–18°40′S: Journal of Geophysical Research, v. 101, p. 8685–8695.

Chadwick, W.W., Scheirer, D.S., Embley, R.W., and Johnson, H.P., 2001, High-resolution bathymetric surveys using scanning sonars: Lava flow morphology, hydrothermal vents, and geologic structure at recent eruption sites on the Juan de Fuca Ridge: Journal of Geophysical Research, v. 106, p. 16,075–16,099.

Cormier, M.-H., and Macdonald, K.C., 1994, East Pacific Rise 18°–19°S: Asymmetric spreading and ridge reorientation by ultrafast migration of axial discontinuities: Journal of Geophysical Research, v. 99, p. 543–564.

Cormier, M.-H., Scheirer, D.S., and Macdonald, K.C., 1996, Evolution of the East Pacific Rise at 16°–19°S since 5 Ma: Bisection of overlapping spreading centers by new, rapidly propagating ridge segments: Marine Geophysical Researches, v. 18, p. 53–84.

Dekov, V.M., and Kuptsov, V.M., 1992, Late Quaternary rates of accumulation of metal-bearing sediments on the East Pacific Rise: Oceanology, v. 32, p. 94–101.

Embley, R.W., Lupton, J.E., Massoth, G.J., Urabe, T., Tunnicliffe, V., Butterfield, D.A., Shibata, T., Okano, O., Kinoshita, M., and Fujioka, K., 1998, Geological, chemical, and biological evidence for recent volcanism at 17.5°S: East Pacific Rise: Earth and Planetary Science Letters, v. 163, p. 131–147.

Hooft, E.E.E., Detrick, R.S., and Kent, G.M., 1997, Seismic structure and indicators of magma budget along the southern East Pacific Rise: Journal of Geophysical Research, v. 102, p. 27,319–27,340.

Hurst, S.D., Karson, J.A., and Verosub, K.L., 1994, Paleomagnetism of tilted dikes in fast spread oceanic crust in the Hess Deep Rift: Implications for spreading and rift propagation: Tectonics, v. 13, p. 789–802.

Johnson, H.P., Hautala, S.L., Tivey, M.A., Jones, C.D., Voight, J., Pruis, M.J., Garcia-Berdeal, I., Gilbert, L.A., Bjorklund, T., Fredericks, W., Howland, J., Tsurumi, M., Kurakawa, T., Nakamura, K.-I., O'Connell, K., Thomas, L., Bolton, S., and Turner, J., 2002, Survey studies hydrothermal circulation on the northern Juan de Fuca Ridge: Eos (Transactions, American Geophysical Union), v. 83, p. 73, 78–79.

Lagabrielle, Y., and Cormier, M.-H., 1999, Formation of large summit troughs along the East Pacific Rise as collapse calderas: An evolutionary model: Journal of Geophysical Research, v. 104, p. 12,971–12,988.

Macdonald, K.C., 1982, Mid-ocean ridges: Fine scale tectonic, volcanic and hydrothermal processes within the plate boundary zone: Annual Review of Earth and Planetary Sciences, v. 10, p. 155–190.

Marchig, V., Erzinger, J., and Heinze, P.M., 1986, Sediment in the black smoker area of the East Pacific Rise (18.5°S): Earth and Planetary Science Letters, v. 79, p. 93–106.

Perfit, M.R., and Chadwick, W.W., 1998, Magmatism at mid-ocean ridges: Constraints from volcanological and geochemical investigations, *in* Buck, W.R., et al., eds., Faulting and magmatism at mid-ocean ridges: American Geophysical Union Geophysical Monograph 106, p. 59–115.

Renard, V., Hékinian, R., Francheteau, J., Ballard, R.D., and Bäcker, H., 1985, Submersible observations at the axis of the ultra fast spreading East Pacific Rise (17°30′ to 21°30′S): Earth and Planetary Science Letters, v. 75, p. 339–353.

Ryan, W.B.F., Cormier, M.-H., Bradley, A.M., Yoerger, D.R., and Singh, H., 1999, Branching and confluence of axially-fed lava channels on the crest of the East Pacific Rise at 17°28′S [abs.]: Eos (Transactions, American Geophysical Union), v. 80, p. F1074.

Scheirer, D.S., and Macdonald, K.C., 1993, Variations in cross-sectional area of the axial ridge along the East Pacific Rise: Evidence for the magmatic budget of a fast spreading center: Journal of Geophysical Research, v. 98, p. 7871–7885.

Shah, A.K., Cormier, M.-H., Ryan, W.B.F., Jin, W., Sinton, J.M., Bergmanis, E.C., Carlut, J., Bradley, A.M., and Yoerger, D.R., 2003, Episodic dike swarms inferred from near-bottom magnetic anomaly maps at the southern East Pacific Rise: Journal of Geophysical Research, v. 108, DOI 10.1029/2001JB000564.

Sinton, J.M., Bergmanis, E.C., Rubin, K.H., Batiza, R., Gregg, T.K.P., Grönvold, K., Macdonald, K.C., and White, S.M., 2002, Volcanic eruptions on mid-ocean ridges: New evidence from the superfast spreading East Pacific Rise, 17°–19°S: Journal of Geophysical Research, v. 107, DOI 10.1029/2000JB000090.

White, S.M., Macdonald, K.C., and Haymon, R.M., 2000, Basaltic lava domes, lava lakes, and volcanic segmentation on the southern East Pacific Rise: Journal of Geophysical Research, v. 105, p. 23,519–23,536.

Yoerger, D.R., Bradley, A.M., Walden, B.B., Cormier, M.-H., and Ryan, W.B.F., 2000, Fine-scale seafloor survey in rugged deep-ocean terrain with an autonomous robot, International Conference on Robotics and Automation: San Francisco, Institute of Electrical and Electronics Engineers, p. 1787–1792.

Manuscript received 5 September 2002
Revised manuscript received 12 March 2003
Manuscript accepted 19 March 2003

Printed in USA